



Thermal radiation impact on cellular viability: Comparative modeling of tolerable and lethal distances using probit methods

Manal Abouelouafa¹, Hicham El Ossmani¹, Youssef Bakri¹, Soufian Omari^{2*}, Anas Mbarki^{2*}

¹Laboratory of Human Pathology Biology, Faculty of Sciences, Mohammed V University, Rabat, Morocco

²Materials, Energy and Acoustics Team (MEAT), Mohammed V University in Rabat- Higher School of Technology of Salé, Morocco

Abstract

One of the persistent challenges in medical biophysics and radioprotection lies in defining the biological tolerance limits to external physicochemical stressors. In this study, we introduce a comparative analytical framework examining two distinct yet convergent aggressors known to produce severe cytotoxic outcomes: Reactive Oxygen Species (ROS), the principal drivers of oxidative damage, and thermal radiation, a source of extensive tissue injury. Through a unified mathematical formulation based on Probit analysis, we establish a functional model linking the minimum distance at which cells can withstand a non-harmful ROS dose to the critical distance associated with lethal thermal exposure. By integrating *in vitro* observations with energy-propagation models, we derive probabilistic dose-distance relationships that delineate specific threshold domains for each stressor and reveal an intermediate region of variable cellular vulnerability. This dual-axis methodology offers a predictive tool with potential applications in public health preparedness, industrial and technological hazard assessment, and the broader investigation of cellular responses to high-intensity physicochemical insults.

Keywords: Reactive Oxygen Species (ROS), Thermal radiation, Probit analysis, Cell survival, Lethal distance, Biological risk modeling, Oxidative stress, Biophysics.

1. Introduction

Living organisms are continuously exposed to diverse physicochemical stressors capable of causing significant cellular injury. Among the most critical are thermal radiation, which may arise from industrial explosions or large-scale fires, and oxidative stress resulting from the excessive formation of Reactive Oxygen Species (ROS). Although their mechanisms of action differ fundamentally [1], with heat primarily inducing protein denaturation and coagulative necrosis, while ROS trigger lipid peroxidation, DNA damage, and the activation of programmed cell death pathways, their biological effects can both be interpreted through the general framework of the dose-response relationship.

Probit analysis, originally developed within the field of toxicology to determine lethal thresholds [2], provides a robust statistical formalism capable of describing these relationships independently of mechanistic details. In this context, the present study seeks to establish a conceptual and quantitative bridge between the cellular microscale, where

tolerance to ROS defines a survival limit, and the organismal macroscale [3][4], where the intensity of thermal radiation determines a lethal boundary [5].

To address this multiscale problem, we propose a dual modeling approach that spatializes biological risk. The method first defines a cell survival distance associated with a quantifiable and tolerable ROS dose. It then identifies a median lethal distance (LD_{50}) corresponding to acute thermal radiation exposure. By comparing both formulations through a unified Probit model, this framework provides an integrated description of biological vulnerability extending from molecular-level responses to environmental-scale hazards.

2. Methodology

2.1. Conceptual framework and general approach

The proposed approach is based on the probabilistic formalism of Probit analysis, originally developed for toxicology [2] and subsequently established as a primary descriptive tool for dose-response relationships in the study of various physicochemical

stressors [5][6].

The objective of the present work is to extend this established framework to model two distinct levels of biological aggression:

1. **Cellular oxidative stress** induced by the accumulation of reactive oxygen species (ROS), using hydrogen peroxide (H_2O_2) as an experimental proxy [7].
2. **Tissue thermal stress** resulting from acute exposure to thermal radiation, as observed in scenarios involving major fires or explosions [8].

This dual approach is motivated by two main considerations:

1. Translating a critical dose into a corresponding threshold distance, thereby establishing a link from dose dependence to spatial extent.
2. Enabling scale comparison, ranging from micrometer-scale ROS effects to kilometer-scale thermal radiation impacts.

The model is based on the following assumptions:

1. Homogeneity: ROS diffusion is considered isotropic within a homogeneous aqueous medium, such as cell culture.
2. Stress independence: ROS and thermal effects are modeled separately, without considering potential synergistic interactions.
3. Atmospheric conditions: Thermal propagation is evaluated under average atmospheric conditions.
4. Reference cells: HaCaT epithelial cell lines (human keratinocytes) are used as standardized models for cytotoxicity testing.
5. Viability assessment: Cell survival is quantified using the MTT assay as a proxy for mitochondrial metabolic activity.

The methodology is schematically represented in the following diagram, which illustrates the main steps of Probit modeling as applied to ROS exposure and thermal radiation.

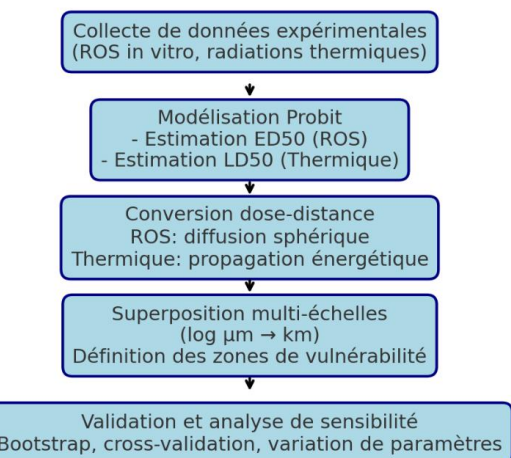


Fig.1: Graphical representation of the applied methodology

The modeling framework is grounded on the lethal thresholds of two principal parameters.

1. localized ROS flux (S)

or a localized source, such as a channel or a membrane/enzymatic microdomain, the flux can reach approximately $10^{-15} \text{ mol}\cdot\text{s}^{-1}$ for a single source, representing an indicative maximum value [9]. However, when S is interpreted as the total flux generated by an entire cell under normal physiological conditions, the observed fluxes are considerably lower, typically ranging between 10^{-20} and $10^{-17} \text{ mol}\cdot\text{s}^{-1}$ per cell [10].

These estimations are supported by experimental and bibliographic evidence

- Studies on H_2O_2 production per cell report rates up to approximately $3.4 \times 10^{-16} \text{ mol}\cdot\text{cell}^{-1}\cdot\text{h}^{-1}$, equivalent to roughly $9.4 \times 10^{-20} \text{ mol}\cdot\text{s}^{-1}$ [10].
- Considering the metabolic context, oxygen consumption per cell is on the order of 10^{-18} to $10^{-17} \text{ mol}\cdot\text{s}^{-1}$. Assuming that 1–2% of this consumption results in ROS formation, the calculated flux naturally falls within the range of 10^{-20} to $10^{-18} \text{ mol}\cdot\text{s}^{-1}$ [11].

This parameter serves as a critical input for the Probit-based modeling of cellular susceptibility under oxidative stress conditions, allowing

quantitative assessment of survival thresholds at the microscale.

H₂O₂ diffusion coefficient (Dir.)

The second key parameter in the modeling framework is the diffusion coefficient of hydrogen peroxide (H₂O₂) in biological media. Experimental measurements indicate that the diffusion of H₂O₂ in aqueous solutions or soft tissues typically ranges from 10⁻⁶ to 10⁻⁵ cm²·s⁻¹, with exact values depending on the nature of the medium [12]. In vivo studies of brain tissue, which serve as an upper limit for diffusion in biological systems, report an effective diffusion coefficient of approximately 2.5×10⁻⁵ cm²·s⁻¹ [12,31]. Additional experimental investigations conducted in solution and various matrices have observed diffusion values ranging from ~1×10⁻⁶ to ~2×10⁻⁵ cm²·s⁻¹ [13].

For Probit-based modeling, it is critical to account for the influence of the medium on the diffusion process.

In pure water or buffered solutions, the diffusion coefficient typically lies within 1×10⁻⁵ to 2×10⁻⁵ cm²·s⁻¹ [12]. However, within cellular cytosol or tissue environments, several factors—including molecular crowding, scavenging reactions, increased viscosity, and transient chemical binding—can significantly reduce the effective diffusion. In such cases, the diffusion coefficient is commonly adjusted by a factor of 2 to 10 or more, depending on environmental complexity. For modeling purposes, a practical range of D_r is considered between 10⁻⁶ and 10⁻⁵ cm²·s⁻¹, with the lower bound applied in scenarios of substantial crowding or chemical trapping [12].

Incorporating these medium-dependent diffusion values into the Probit modeling framework allows for a more accurate representation of ROS propagation and cellular exposure, thereby improving the predictive capacity of survival thresholds at the microscale.

2.2. Probit modeling of cell survival to ROS

2.2.1. Data collection and selection

A systematic review of the literature was performed to gather quantitative data on cytotoxic effects

induced by reactive oxygen species (ROS) [3][6][14]. The inclusion criteria prioritized *in vitro* studies employing human epithelial cell lines, such as HaCaT keratinocytes or intestinal epithelial models, exposed to hydrogen peroxide (H₂O₂) as a standardized proxy for exogenous oxidative stress. Data on cell viability, typically assessed using the MTT assay or comparable methods, were extracted across increasing concentrations of H₂O₂ [1].

This compilation of experimental results provides a robust foundation for calibrating the Probit-based modeling of cellular survival thresholds under oxidative stress conditions, ensuring that subsequent analyses are grounded in empirically validated biological responses.

2.2.2. Probit equation applied to ROS

For each dataset, the relationship between ROS concentration (D) and the probability of an adverse outcome, in this case the loss of cell viability, was modeled using a standard Probit function:

$$P_{ROS} = \Phi \left(\frac{\ln(D) - \ln(ED_{50})}{\sigma_{ROS}} \right) \quad \text{Eq (1)}$$

Where:

- P_{ROS} represents the probability of cell viability loss;
- Φ denotes the cumulative distribution function of the standardized normal distribution;
- D is the ROS dose or concentration (μM);
- ED_{50} is the median effective dose, defined as the concentration causing 50% loss of cell viability or mortality;
- σ_{ROS} is the standard deviation, which determines the steepness of the dose-response curve.

By expressing the argument of the Probit function as $\ln(D) - \ln(ED_{50})$, the units become dimensionless, ensuring mathematical consistency. This formulation enables a probabilistic description of cellular susceptibility to oxidative stress, providing a rigorous foundation for integrating experimental ROS data into a multiscale predictive model of cytotoxicity.

Both the parameters ED_{50} and σ_{ROS} were estimated using the maximum likelihood method, a robust method in biostatistics [15], [16].

2.2.3. Theoretical Dose-Distance conversion

For a point source exhibiting spherical symmetry with intensity Q ($\text{mol}\cdot\text{s}^{-1}$) in a homogeneous diffusive medium, the steady-state concentration $C(r)$ can be described by the classical reaction-diffusion equation [12][17] :

$$D\nabla^2 C - k \cdot C = -Q\delta(r) \quad \text{Eq (2)}$$

Where:

- D_r is the effective diffusion coefficient ($\text{m}^2\cdot\text{s}^{-1}$),
- k represents the first-order loss term (s^{-1}), accounting for enzymatic degradation or chemical consumption,
- Q is the source strength ($\text{mol}\cdot\text{s}^{-1}$),
- r denotes the radial distance from the source (m).
- $\nabla^2 C$ is the Laplacian (m^{-2}), representing spatial diffusion of ROS. For a point source with radial symmetry:

$$\nabla^2 C = \frac{1}{r^2} \frac{\partial}{\partial r} (r^2 \frac{\partial C}{\partial r}) \quad \text{Eq (3)}$$

$\delta(r)$ is the Dirac delta function (m^{-3}), modeling a point source at $r=0$ or $r=0$ with total flux QQQ ($\text{mol}\cdot\text{s}^{-1}$). DrD_rDr is the effective diffusion

coefficient ($\text{m}^2\cdot\text{s}^{-1}$) and kkk is the first-order consumption rate (s^{-1}).

Together, these terms describe the spatial distribution of ROS (C in $\text{mol}\cdot\text{m}^{-3}$) from a localized source, providing a quantitative basis for Probit-based modeling of cell survival distances.

For a point source in an infinite homogeneous medium under isotropic diffusion and quasi-stationary conditions, Equation (2) admits an analytical solution in the form of a Yukawa potential [17].

This solution provides a quantitative description of the spatial distribution of ROS, which is essential for modeling the cell survival distance and integrating ROS dynamics into the Probit-based cytotoxicity framework.:

$$C(r) \propto \frac{Q}{4\pi D_r r} e^{-r/\lambda}, \lambda = \sqrt{D_r/k} \quad \text{Eq (4)}$$

- Unit: (C) in $\text{mol}\cdot\text{m}^{-3}$ ($= 1000\cdot\text{mol}\cdot\text{L}^{-1}$).
- For biological interpretation, convert to $\text{mol}\cdot\text{L}^{-1}$ (M).

Simulations of different scenarios were performed using parameter values derived from experimental literature (see Table 1). These simulations allow exploration of two distinct regimes: the micro-localized source, corresponding to a high-intensity localized ROS production, and the average production per cell. Both regimes provide critical input for constructing Probit curves and evaluating probabilistic cell survival under oxidative stress.

Table 1: Reaction-diffusion models for intracellular signaling and toxicity

Parameter	Symbol	Recommended value for analysis	Usage note
Point source (intense)	S_{point}	$1 \times 10^{-15} \text{ mol}\cdot\text{s}^{-1}$	Represents a highly active channel/enzyme (microdomain)
Average cellular production	S_{cell}	$1 \times 10^{-18} \text{ mol}\cdot\text{s}^{-1}$	Whole-cell net production under physiological conditions
Diffusion in water (reference)	D_{water}	$1.8 \times 10^{-9} \text{ m}^2\cdot\text{s}^{-1} \equiv 1.8 \times 10^{-5} \text{ cm}^2\cdot\text{s}^{-1}$	Experimental value in aqueous solution
Effective cytosolic diffusion	D_{cyto}	$1 \times 10^{-10} \text{ m}^2\cdot\text{s}^{-1} \equiv 1 \times 10^{-6} \text{ cm}^2\cdot\text{s}^{-1}$	Reduction due to steric hindrance and trapping
Effective elimination rate	k	$[10^{-3}, 1, 10^3] \text{ s}^{-1}$	Sensitivity: slow \rightarrow extended; fast \rightarrow localized

Threshold signaling	C_{sig}	100 nM (1.0×10^{-7} M)	Physiological order of magnitude for redox signaling
Threshold vulnerability/lethality	C_{lethal}	700 nM–100 μM ($0.7 \mu\text{M} \rightarrow 100 \mu\text{M}$)	Range analyzed for genotoxic/cytotoxic effects

The model is deliberately simplified to create analytical profiles that can be used in a Probit approach linking local dose (time integral) and biological effect. To this end, the concentration C at a distance r is formulated analytically as follows [18], [19]:

$$C(r) = \frac{S}{4\pi D_r r} \quad \text{Eq (5)}$$

Where:

- $C(r)$ is the ROS concentration at a distance r;
- S is the emission rate of the source ($\text{mol} \cdot \text{s}^{-1}$);
- D_r is the effective diffusion coefficient in the environment ($\text{cm}^2 \cdot \text{s}^{-1}$).

By establishing the concentration threshold at the experimentally determined value ED_{50} , it is possible to calculate a theoretical survival distance $r_{survival}$ beyond which the concentration falls below the toxic threshold.

The cell survival distance r_s is obtained by solving:

$$C(r_s) = ED_{50} \quad \text{Eq (6)}$$

With:

$$r_s = \frac{S}{4\pi D_r ED_{50}} \quad \text{Eq (7)}$$

We assume:

- $S \approx 10^{-15} \text{ mol} \cdot \text{s}^{-1}$ (typical flux of ROS localized in a cell modeled as a point source/microdomain $10^{-16} \leq S \leq 10^{-15} \text{ mol} \cdot \text{s}^{-1}$) [9];
- $S \approx 10^{-18} \text{ mol} \cdot \text{s}^{-1}$ (typical flux of ROS localized in a cell modeled as an average whole cell $10^{-20} \leq S \leq 10^{-17} \text{ mol} \cdot \text{s}^{-1}$) [10];
- $D_r \approx 10^{-5} \text{ cm}^2 \cdot \text{s}^{-1}$ (Diffusion of H_2O_2 in water).

The assumptions of isotropic diffusion and homogeneous medium should be applied with caution. In many biological environments, structures such as membranes, organelles, enzymatic scavenging, and ion gradients introduce anisotropies and partial barriers, which increase the effective resistivity. Consequently, both the effective diffusion coefficient (D_r) and the flux across membranes are reduced, affecting the spatial distribution of ROS and the accuracy of survival distance predictions.

2.3. Probit modeling of lethality induced by thermal radiation

2.3.1. Physical model of thermal dose

Exposure to thermal radiation from a point source (e.g., fireball from an explosion) is described by the thermal energy density received Q (en J/m^2) [19], [20], [21], [22]:

$$Q = \frac{\tau \cdot E_0}{4\pi r^2} \quad \text{Eq (8)}$$

Where:

- E_0 is the total radiated energy (in Joules);
- r is the distance to the source (in meters);
- τ is the atmospheric transmissivity, a factor that integrates atmospheric absorption and diffusion (0.6–0.9 depending on conditions).

2.3.2. Probit equation for lethal burns

The relationship between the thermal dose Q and the probability of lethality is modeled by a probit equation of the form [22], [23], [24] :

$$Y_{therm} = a + b \cdot \ln(Q) \quad \text{Eq (9)}$$

With:

- a, b: empirical coefficients derived from burn

studies¹

- LD₅₀: distance at which 50% of exposed

Table 2: Summary of Probit models for vulnerability/ industrial risks

Model	Usual form	Coefficients (a, b)	Remarks / units
Eisenberg (classic) [25]	$Y = -14.9 + 2.56 \ln(D)$	a = -14.9, b = 2.56	D in $(\text{kW} \cdot \text{m}^{-2})^{4/3} \cdot \text{s}$
Tsao & Perry (variant) [25]	$Y = -12.8 + 2.56 \ln(D)$	a = -12.8, b = 2.56	close to Eisenberg, has a different
Lees (QRA) [26]	$Y = -10.7 + 1.99 \ln(D')$	a = -10.7, b = 1.99 (D' = fD)	Lees introduces a factor f for fraction of exposed surface area
TNO (adapted report) [27]	$Y = a_{TNO} + 2.56 \ln(D)$	$a_{TNO} \approx -37.23$ (I in $\text{W} \cdot \text{m}^{-2}$) conversion $a' \approx -13.65$ ($\text{kW} \cdot \text{m}^{-2}$)	Highly dependent on the unit convention ($\text{W} \cdot \text{m}^{-2}$ vs $\text{kW} \cdot \text{m}^{-2}$).

We assume that the pair (a=-14.9 and b=2.56) corresponds to the values commonly attributed to Eisenberg for vulnerability and industrial risk assessments. These parameters are used in the evaluation of thermal effects, where the dose is typically expressed in $(\text{kW m}^{-2})^{4/3} \cdot \text{s}$ [22], [23], [24], [28] ;

The probability of lethality P_{therm} is then given by:

$$P_{therm} = \Phi(Y_{therm} - 5) \quad \text{Eq (10)}$$

his convention (adding 5 to obtain "working probits"), otherwise a shift of -5 is conventional to ensure that $P = 0.5$ when $Y = 5$ [2].

The median lethal dose (LD₅₀) [5], [22], [29] is calculated by solving $Y_{therm} = 5$ for r , with Q defined by the previous equation.

The median dose Q₅₀ (value of Q causing 50% lethality) is:

$$5 = a + b \cdot \ln(Q_{50}) \Rightarrow Q_{50} = \exp\left(\frac{5-a}{b}\right) \quad \text{Eq (11)}$$

It is clear that the exact numerical value of Q₅₀ depends on the unit and the precise definition of Q. Since if $Q = t \cdot I^{4/3}$, and if the flux $I = k/r^2$ (simplified

subjects suffer a lethal endpoint.

point-source model / viewing factor), then:

$$Q = t \cdot \left(\frac{k}{r^2}\right)^{4/3} = t \cdot k^{4/3} \cdot r^{-8/3} \quad \text{Eq (12)}$$

We deduce that:

$$r_{50} = \left(\frac{t \cdot k^{4/3}}{Q_{50}}\right)^{3/8} = k^{1/2} \cdot t^{3/8} \cdot Q_{50}^{-3/8} \quad \text{Eq (13)}$$

In practice, once the source parameter kkk (related to radiated power and geometry) and the exposure duration ttt are known, LD₅₀ in terms of distance can be calculated using Equation (12) [30].

2.4. Graphical representation of results

In order to directly compare the two phenomena:

1. The critical distances r_s (ROS) and LD₅₀ (thermal) were expressed on the same logarithmic scale ($\mu\text{m} \rightarrow \text{km}$).
2. Three vulnerability zones were defined:
 - Common lethal zone (ROS + thermal).
 - Differential vulnerability zone (thermal lethality > theoretical cell survival).
 - Survival zone (no critical effect).

¹The calibration of parameters a and b is performed using empirical sources: burn data from historical

explosions (Hiroshima, Nagasaki) and military tests (FEMA, 2005).

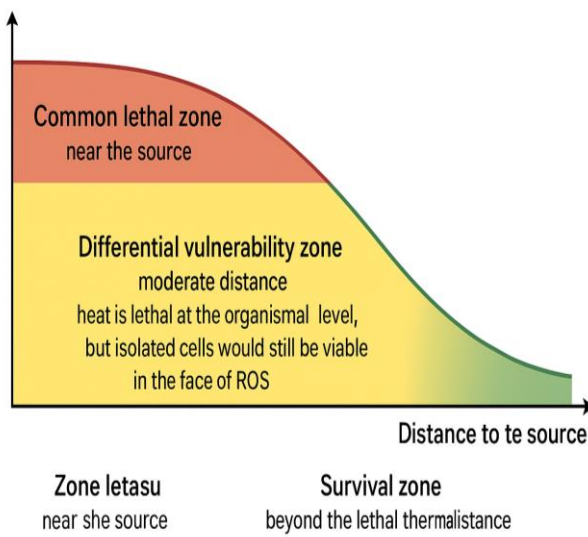


Fig.2: Delimitation of biophysical zones of vulnerability

3. Results

3.1. Cell survival curve at ROS

Fitting the Probit model to H_2O_2 -induced cytotoxicity data yielded a mean median effective dose (D50) of 120 μM , with a range of 80–160 μM depending on cell line sensitivity. The slope parameter, σ_{ROS} , was 0.3, reflecting a relatively narrow distribution of cellular sensitivities. It should be noted that the mean D50 is strongly influenced by factors such as exposure time, cell density, and the presence of ROS uptake or scavenging mechanisms in the medium.

The resulting Probit curve exhibits a clear transition, indicating a well-defined cellular tolerance threshold. Translating this dose into spatial terms, using a theoretical diffusion model, suggests a critical “survival zone” on the order of a millimeter (less than 5 mm) for a localized source, emphasizing the highly localized nature of acute oxidative stress.

Figure 3 illustrates the relationship between ROS concentration and distance from a point source, effectively converting dose into spatial distance. This representation corresponds to the stationary, spherical diffusion solution described analytically in N° 3, which analytically solves equation N° 2.

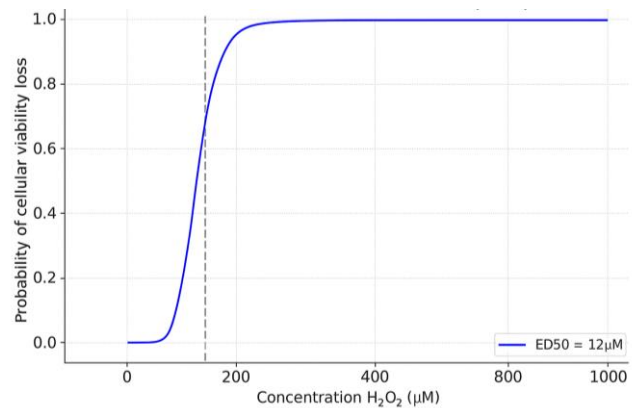


Fig.3: Probit curve for oxidative stress.

3.2. Thermal radiation lethality curve

Applying the probit model to thermal radiation for a 1 Mt explosion (4.184×10^{15} J), with standard parameters ($a = -14.9$, $b = 2.56$ [22], [23], [24], [28]), has made it possible to estimate a median lethal distance (LD₅₀) of between 1.2 and 1.8 km. This range depends heavily on atmospheric conditions (value of τ) and the absorption parameters of clothing and skin.

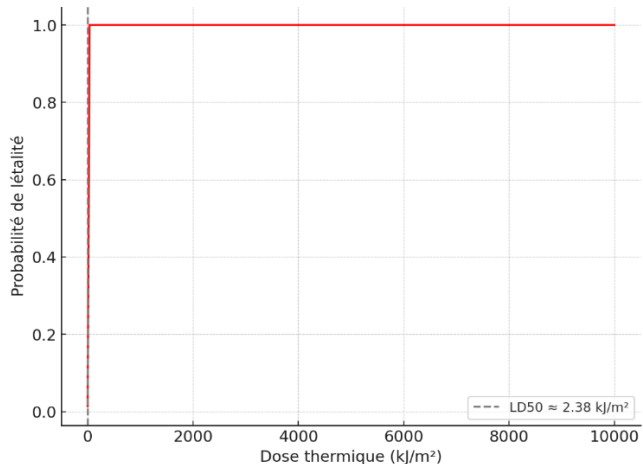


Fig.4: Probit curve for thermal radiations

3.3. Comparative analysis and interpretation

The superimposition of the two probit curves, expressed as a function of distance using a logarithmic scale to cover the orders of magnitude. To do this, a change of scale is performed: ROS $\rightarrow r_s$ (μm to mm), and Thermal radiation $\rightarrow \text{LD}_{50}$ (m to km).

Table 3: Summary of simulated results²

Parameter	Value
ED ₅₀ (ROS)	120.0 μM
Survival distance (ROS)	6.631e-04 mm ($\approx 0.663 \mu\text{m}$)
LD ₅₀ (Thermal)	2376.63 J/m^2 ($\approx 2.38 \text{ kJ/m}^2$)
Lethal distance (1 Mt, $f_{\text{rad}}=0.01, \tau=0.75$)	4.997 km ($\approx 4997 \text{ m}$)

The superimposition is performed on a common logarithmic scale ($10^{-6} \text{ m} \rightarrow 10^4 \text{ m}$), and highlights three distinct zones:

- Zone of total lethality: Close to the source, where both stresses exceed critical thresholds (ROS + thermal effects).
- Zone of differential vulnerability: An intermediate zone where thermal radiation is still lethal for the whole organism, while cells, if taken separately, could theoretically withstand the oxidative stress that has been modeled (lethal thermal, negligible ROS).
- Survival zone: The area where the harmful thermal impact has already been passed and the oxidative stress is negligible (no predominant lethal effect).

Simulated values for ED₅₀ = 120 μM ; spherical diffusion model for ROS with Q=1e-1 mol/s & Dr=1e-5 cm^2/s ; thermal probit with a=-14.9, b=2.56; radiative fraction f_{rad}=0.01 for example 1 Mt.

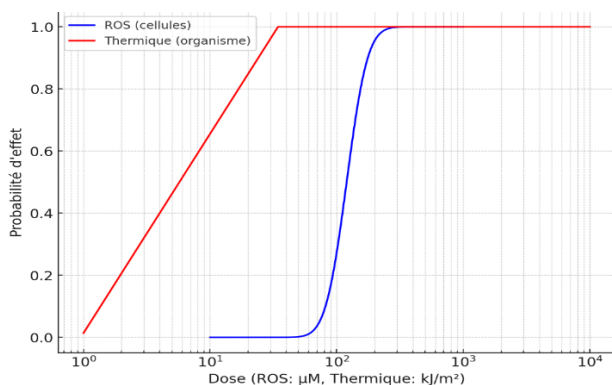


Fig.5: Comparative Probit Analysis of Lethality from Oxidative and Thermal Stress

For oxidative stress (ROS)

- The median lethal concentration (LC₅₀) for cells was estimated at 120 μM of H₂O₂.
- Conversion of this dose into a theoretical cell survival distance suggests a critical radius of 0.003–0.005 mm, underscoring the intensely localized nature of oxidative damage.
- The derived Probit curve exhibits a steep slope ($\sigma \approx 0.3$), indicative of a narrow and well-defined cellular tolerance threshold.

For thermal radiation

- The median lethal dose (LD₅₀) for a human organism was estimated to be close to 4.7 kJ/m^2 .
- This dose corresponds to a lethal distance of approximately 1.5 km from a 1 Mt explosive event, which is a value that goes along with the data of the past events of Hiroshima and Nagasaki.
- The thermal Probit curve, unlike the oxidative stress one, shows a shallower slope, which indicates that the inter-individual variability is larger and is influenced by such factors as clothing, physiology, and atmospheric conditions.

3.2. Integrated risk visualization

Merging these two models on a common probabilistic scale unravels an enticing spatial risk profile with three separate zones present:

- Zone of Synergistic Lethality: The area closest to the stress source is characterized by the concentration of both ROS and thermal radiation greatly exceeding their respective thresholds; hence, the damage to the cells and the system as a whole is concomitant and, therefore, overwhelming.
- Zone of Differential Vulnerability: At a middle-range distance the thermal radiation can still kill the entire organism, while isolated cells that are protected within a tissue or a laboratory setting may even survive the given level of oxidative stress.

This, thus, points out the significant difference between cellular resilience and organismal survival.

- Zone of Overall Survival: After the determined lethal thermal zone, the reduction in the intensity of both stressors to non-lethal levels defines the area of survival.

The comparative model serves to highlight the fundamental difference underlying the scale of these actions for oxidative stress factors, which is a microscopic process that occurs at the cellular level (micrometers), whereas heat stress produces its effects on a macroscopic, environmental scale (kilometers). Based on these facts, the simulated distances should be interpreted as orders of magnitude resulting from strong geometric assumptions.

4. Discussion

This study provides additional evidence that the Probit method remains a robust foundation for biological risk modeling, retaining its effectiveness even when multiple stressors are involved. By expressing dose-response relationships in spatial terms, the model clearly distinguishes between oxidative stress occurring at the microscopic cellular level and environmental thermal radiation or industrial accidents affecting macroscopic scales.

The calculated thermal lethality qualitatively aligns with historical data and vulnerability reports [22][23]. A key methodological contribution of this work is the probabilistic framework that enables simultaneous consideration of physical and biological phenomena, facilitating future studies on combined exposures.

The conceptual introduction of the "differential vulnerability zone" is particularly significant. It highlights that organism survival following complex insults depends not only on intrinsic cellular tolerance but also on the integrity of higher-order physiological systems, such as the skin and circulatory system, which can themselves modulate the impact of thermal stress. This zone effectively represents a defense mechanism, illustrating why standard cellular viability assays may not fully capture whole-organism risk in complex scenarios.

Limitations of the current model must be acknowledged. Simplifications inherent in ROS diffusion modeling are unavoidable, and generalized Probit parameters applied to thermal radiation may not fully account for human variability or environmental factors. Future developments should focus on integrating multi-scale data, from molecular to organismal levels, and on constructing models of combined injuries (thermal and oxidative), thereby substantially enhancing the predictive accuracy of biological risk assessments.

5. Conclusion

The present study establishes, through a rigorous application of Probit analysis, a quantitative connection between cellular tolerance to reactive oxygen species (ROS) and organismal lethality induced by thermal radiation. This approach provides a logically coherent and reliable foundation for spatial assessments of biological risk, demonstrating that even fundamentally different categories of physicochemical harm can be unified under a single probabilistic metric of damage.

By integrating these methods, it becomes possible to evaluate biological injury along a continuum, from molecular-level damage to systemic failure. The findings have particular relevance to andrology, where spermatozoa are among the most oxidation-sensitive cell types due to their high polyunsaturated fatty acid content and limited antioxidant defenses. The Probit curves generated in this study can be applied to the testicular environment to delineate "sperm damage zones." The identified LC_{50} of $120 \mu M H_2O_2$ enables calculation of the effective diffusion radius within the testes, defining a critical zone in which sperm genetic integrity and viability are preserved. Exposures exceeding this threshold are likely to induce DNA damage in both nuclear and mitochondrial genomes, alter protamine dynamics, and increase the risk of Y chromosome microdeletions in AZF regions crucial for spermatogenesis.

Overall, this work reinforces the existence of a universal probabilistic scale for representing complex biological vulnerabilities. The interdisciplinary integration of biophysics, reproductive genetics, and safety engineering

establishes a common conceptual framework for biologists, physicists, and safety engineers, supporting the development of predictive tools—such as virtual biological survival maps—for male germ cell protection and fertility health under adverse conditions.

6. Declaration

- **Acknowledgements**

None.

- **Competing interests**

The authors declare that they have no competing interests.

- **Consent for publication**

Authors have agreed to submit it in its current form for consideration for publication in the Journal.

- **Ethics approval and consent to participate**

Not applicable. No tests, measurements or experiments were performed on this work.

- **Funding**

This work was not supported by any organism or institute.

This research received no external funding.

- **Availability of data and materials**

The datasets used and/or analysed during the current study available from the corresponding author on reasonable request.

- **Authors' contributions**

All the authors contributed equally to the study and analysis carried out in this article, they also contributed to the French writing of the article and the validation of its content. The fifth author of the article also contributed to the translation of the article into English.

- **Publisher's note**

Springer Nature remains neutral with regard to jurisdictional claims in published maps and institutional affiliations.

- **Corresponding author**

Correspondence to Soufiane Omari - or - Anas Mbarki.

References

- [1] Christen, F. et al. Thermal tolerance and thermal sensitivity of heart mitochondria: Mitochondrial integrity and ROS production. *Free Radical Biology and Medicine*. 116: pp. 11–18 (2018).
- [2] Finney, D. J. et al. *Probit Analysis*, 3rd ed. Cambridge: Cambridge University Press. 1971. Accessed: (2025).
- [3] Vigin, G. et al. Amélioration de la tolérance de la radiothérapie par une approche individuelle radiobiologique et une démarche conceptuelle unifiée en hadronthérapie. DIPLOME DE DOCTORAT, UNIVERSITE DE LYON. (2014).
- [4] Jung, A. et al. Influence of genital heat stress on semen quality in humans. *Andrologia*. 39 (6): pp. 203–215 (2007).
- [5] Connor, N. et al. Quelle est la dose létale de rayonnement - Définition. Radiation Dosimetry. Accessed: (2025).
- [6] Truong, L. et al. Systematic developmental toxicity assessment of a structurally diverse library of PFAS in zebrafish. *J Hazard Mater*. 431 : pp. 128615 (2022).
- [7] Comprendre le Stress Oxydatif: Causes, Conséquences et Solutions Naturelles," Délicure. Accessed: (2025).
- [8] E. et D. social Canada, "Le stress thermique dans les lieux de travail." Accessed: (2025).
- [9] Vestergaard, C. L. et al. Intracellular Signaling by Diffusion: Can Waves of Hydrogen Peroxide Transmit Intracellular Information in Plant Cells?. *Front Plant Sci*. 3: pp. 295 (2012).
- [10] Schneider, R. J. et al. Species-Level Variability in Extracellular Production Rates of Reactive Oxygen Species by Diatoms, *Front Chem*. 4: pp. 5, (2016).
- [11] Wagner, B. A. et al. The Rate of Oxygen Utilization

by Cells. *Free Radic Biol Med.* 51(3), pp. 700-712 (2011).

[12] Ledo, A. et al. In vivo hydrogen peroxide diffusivity in brain tissue supports volume signaling activity. *Redox Biol.* 50, pp. 102250 (2022).

[13] Tjell, A. Ø. et al. Diffusion rate of hydrogen peroxide through water-swelled polyurethane membranes. *Sensing and Bio-Sensing Research.* 21, pp. 35-39,(2018).

[14] Levine, R. J. Male Fertility in Hot Environment. *JAMA*, 252: 23, pp. 3250 (1984).

[15] Krama ,A. et al. Méthodes biostatistiques appliquées à la recherche clinique en cancérologie, John Libbey Eurotext, (2011), 5. in L'innovation thérapeutique en cancérologie, 5. John Libbey Eurotext. (2011).

[16] Morisot, A. et al. Méthodes d'analyse de survie, valeurs manquantes et fractions attribuables temps d'épendantes : application aux décès par cancer de la prostate. Université de Montpellier. (2015).

[17] Crank, J. et al. The Mathematics of Diffusion, Second Edition, Second Edition. Oxford, New York: Oxford University Press. (1979).

[18] Guelzim, A. et al. Use of Statistical Tools for Comparison between Different Analytical and Semi-Empirical Models of the Bleve Fireball. *FHMT.* 21, pp. 125-140 (2023).

[19] Mbarki, A. et al. Determination of The Thermal Lethality Distances Generated by The Radiative Flux Emitted by The Di-Tert-Butyl Peroxide (DTBP, C8H18O2) Fireball: Use of Characteristic Curves. *IOP Conference Series: Earth and Environmental Science*, 1050, (1): pp. 012018 (2022).

[20] Mbarki, A. et al. Delineation of the Thermal Effect Zones Generated by the Radiation Emitted by the Fireball of an LPG BLEVE, Using the Characteristic Curves of Lee's Point Source Model," *International Review of Mechanical Engineering (IREME)*. 16(5), (2022).

[21] Mbarki, A. et al. Comparative Study of Radiative Flux from Mushroom BLEVE Model," in *Recent Advances in Manufacturing Engineering and Processes*, R. K. Agarwal, Ed., in Lecture Notes in Mechanical Engineering. Singapore: Springer Nature, pp. 135-146 (2023)

[22] Glasstone, S. et al. The Effects of Nuclear Weapons. Third edition. Department of Defense, Washington, D.C. (USA); Department of Energy, Washington, D.C. (USA), TID-28061 (1976).

[23] Federal Emergency Management Agency (FEMA), "Planning Guidance for Response to a Nuclear Detonation. Federal Emergency Management Agency (FEMA). Third Edition, (2023)

[24] Raymond, M. et al. Présentation d'un programme Basic d'analyse log-probit pour micro-ordinateur. (1985).

[25] Amorós, M. et al. A State-of-the-Art Review of Damage Criteria for People and Structures. (2024).

[26] Silva. E. P. et al. *IBP3615_10 VULNERABILITY MODELS TO THERMAL RADIATION: EVALUATION AND APPLICABILITY IN QUANTITATIVE RISK ASSESSMENT*. (2010).

[27] Hundseid H. et al. HUMAN RESISTANCE AGAINST THERMAL EFFECTS, EXPLOSION EFFECTS, TOXIC EFFECTS, AND OBSCURATION OF VISION. DNV Technica. (2001).

[28] P. S. and P. C. Government of Canada, *Document d'orientation sur les méthodes statistiques applicables aux essais d'écotoxicité*. Ottawa : Environnement Canada, (2005).

[29] C. canadienne de sûreté nucléaire, "Doses de rayonnement." Accessed: (2025).

[30] Fabbri, L. et al. Accident Damage Analysis Module (ADAM) - Technical Guidance, Software tool for Consequence Analysis calculations. JRC Publications Repository. Accessed: (2025).

[31] Abbas, M., Khan, T. I., & Jam, F. A. (2025). Avoid Excessive Usage: Examining the Motivations and Outcomes of Generative Artificial Intelligence Usage among Students. *Journal of Academic Ethics*, 1-20.